Local Structure and Magnetic Properties of FeMnAl Nanocrystalline and Amorphous Alloys

by Kontan Tarigan

Submission date: 07-Apr-2019 02:27PM (UTC+0700)
Submission ID: 1107313931
File name: 2011-_FeMnAl_t_--Advanced_Materials_Research_Vol._277.pdf (464.47K)
Word count: 3191
Character count: 16754

Advanced Materials Research Vol. 277 (2011) pp 100-105
Online available since 2011/Jul/04 at www.scientific.net

doi:10.4028/www.scientific.net/AMR.277.100

Local Structure and Magnetic Properties of FeMnAl Nanocrystalline and Amorphous Alloys

K. Tarigan[1,a], D. S. Yang[2,b], and S. C. Yu[2,c]

[1]Department of Electrical Engineering, Indonesia Institute of Technology, Serpong, 15320, Indonesia

[2]Physics Division, School of Science Education, Chungbuk National University, Cheongju 361-763, South Korea

[3]BK 21 Physics Program and Department of Physics, Chungbuk National University, Cheongju, 361-763, South Korea

[a]kontan_tarigan@yahoo.com, [b]dosyang@chungbuk.ac.kr, [c]scyu@chungbuk.ac.kr

Keywords: $Fe_{55}Mn_{10}Al_{35}$ nanocrystalline and amorphous alloys, structural and magnetic properties

Abstract. The structural and the magnetic properties of nanocrystalline and amorphous $Fe_{55}Mn_{10}Al_{35}$ alloys prepared by the mechanical alloying process are studied as functions of the milling time varying from 1 hr to 48 hrs. Structural analyses based on X-ray diffraction (XRD) and extended X-ray absorption fine structure spectroscopy (EXAFS) reveal that the alloying process took place after 12-hr milling. Nanocrystalline alloys are found until 24-hrs milling, and an amorphous phase afterward. Concerning the magnetic behavior, the data obtained from a vibrating sample magnetometer show that both the magnetization saturation (M_s) and the coercivity (H_c) are dependent strongly on the milling time and the crystallite size. By adjusting the milling time, both appropriate structural transformation and magnetization values are obtained.

Introduction

Amorphous and nanocrystalline magnetic materials have been studied for many applications in industrial products, including transformers, motors, and a wide variety of magnetic components in sensors, power electronics, electrical energy control/management systems, telecommunication equipment and pulse power devices [1]. The wide range of applications arises from the versatile nature of these materials which can provide fast magnetization reversal with minimal magnetic losses. One aspects of the versatility is that materials can be prepared without stoichiometric restrictions characteristic of crystalline materials and by post-fabrication heat treatment. In certain cases, alloys can be designed for specific applications. There are, however, constraints that limit the fabrication of these materials [2]. Amorphous and nanocrystalline materials are a class of their own.

In 1977 Chakrabarti, by using x-ray diffraction, studied the structural phase diagram of the ternary Fe-Mn-Al system for alloys quenched from 1000 °C. The phase diagram of the ternary Fe-Mn-Al system is shown in Figure 1. Dashed lines represent structural transition, exhibiting two principal phases: the γ phase with crystalline fcc structure, which is stable for small Al concentrations and less than 60 at.% of Mn; and the α phase with bcc structure, which is stable for large Al concentration and more than 45 at.% of Fe. The dots represent the experimental results of the ferromagnetic (FM) to paramagnetic (PM) transition in bcc structure [3].

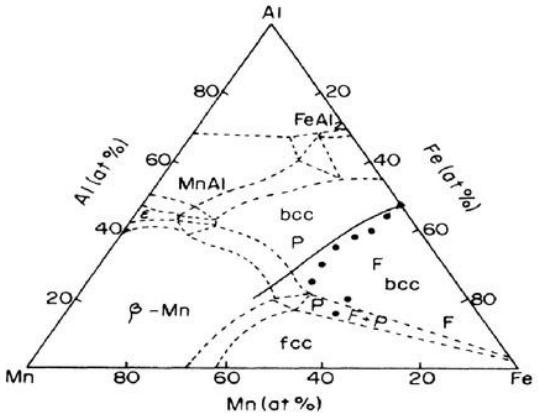

Fig. 1: Phase diagram of the ternary Fe-Mn-Al system [3].

This alloy system is intensively investigated because of the possibility of its application in stainless steels. Although its structural and mechanical properties are well known, its magnetic properties have not been investigated in detail [3].

The alloy system of Fe-Mn-Al belongs to a large family of ternary alloys consisting of two 3*d* transition metals and aluminum. These alloys are of technical and scientific interest because various properties, depending on concentration and heat treatment. It was observed that these alloys can be prepared in crystalline, quasi-crystalline and amorphous states. In many systems solid state reactions appear, such as order or disorder, influencing the physical properties. Especially magnetic properties depend very strongly on the crystal structure, on the phase composition, and on the degree of order in such systems [4]. The system is important due to the presence of competitive and diluted exchange interactions, which are allow to obtain different magnetic phase as paramagnetic, ferromagnetic, spin-glass, reentrant spin-glass and antiferromagnetic phases. The Fe-Mn-Al system which is present depending on composition has a semi-soft magnetic character [5]. Cast Fe–Mn–Al alloys in the bcc disordered phase have been highly studied from the theoretical and experimental point of view, due to the different magnetic phases that can appear as a consequence of the variation in composition and in temperature [6].

The alloys in the Fe-Mn-Al system are characterized by an occurrence of competitive exchange interactions: a given Fe atom is coupled ferromagnetically to its Fe first neighbors and antiferromagnetically to its Mn ones (both the Mn–Fe and the Mn–Mn first-neighbors couplings are antiferromagnetic). The system is also a diluted one since at the Fe and Mn sites, and due to the presence of the nonmagnetic Al atoms, the average number of first neighbors bearing magnetic moment depends on composition (if the alloys have quenched disorder that the number of magnetic first neighbors fluctuates along the crystalline lattice). Thus, the system can be considered a candidate one to exhibit magnetic frustration and spin-glass-like behavior. That phenomenology has, in fact, been shown to occur in the case of disordered $Fe_{0.45}Mn_{0.25}Al_{0.30}$ alloy [7]. A few studies of the ternary Fe–Mn–Al system by mechanical alloying process have been reported in the literature describe the effects of varying the Mn (or Al) concentration on the structural characteristics (the crystal structure and lattice parameters) as well as on the grain size. In general, the magnetic and structural properties of these systems are very similar to those exhibited by powders of melted alloys with the same composition, especially when they are mechanically alloyed for long times [8].

In this work, we prepared and studied structural and magnetic properties of $Fe_{55}Mn_{10}Al_{35}$ alloys by mechanical alloying (MA) with the milling time (t_m) ranging from 1 hr to 48 hrs. Their structural and magnetic properties were then studied by means of X-ray diffraction (XRD), extended X-ray absorption fine structure spectroscopy (EXAFS), and vibrating sample magnetic (VSM).

Experimental

$Fe_{55}Mn_{35}Al_{10}$ nanocrystalline and amorphous alloys were prepared by mechanical alloying using a SPEX 8000 mixer with stainless-steel balls and a stainless-steel vial. The starting mixture of $Fe_{55}Mn_{35}Al_{10}$ was formed by using commercial powders of Fe (53 μm, 99.9%), Mn (75 μm, 99.9%) and Al (53-106 μm, 99.9%). For the milling, the weight ratio of the ball-to-powder was 5:1. $Fe_{55}Mn_{35}Al_{10}$ alloys were mixed and ground for differing times of 1, 6, 12, 24, and 48 hrs. This process was performed in an Ar ambient to avoid oxidation. After the preparation, magnetic measurements were carried out by using a Vibrating Sample Magnetometer (VSM) with magnetic field 2 kOe, we found both of magnetic saturation (M_s) and Coercivity (H_c) from hysteresis loop. Structural data were obtained by using an X-ray diffractometer with the Cu-K_α radiation and Extended X-ray absorption fine structure (EXAFS). Based on XRD data, the crystallite size and the lattice parameters of the samples were estimated by the Scherrer and Bragg equations of the Fe(110) peak. EXAFS data were collected from the 3C1 EXAFS beam line of the Pohang Light Source (PLS). The PLS was operated at an energy of 2.5 GeV and a maximum current of 200 mA. EXAFS spectra were obtained at the Fe K-edge (7112 eV) in the transmission mode at room temperature. After that, the EXAFS data were analyzed by making use of the IFEFFIT software. The structural properties are discussed in connection with the magnetic properties of the alloys.

Results and Discussion

The effects of milling time on $Fe_{55}Mn_{35}Al_{10}$ structural characterization were investigated by XRD and EXAFS. In

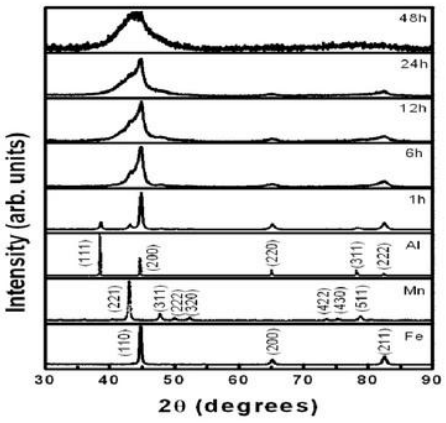

Fig. 2: XRD patterns for $Fe_{55}Mn_{35}Al_{10}$ alloys prepared by ball milling.

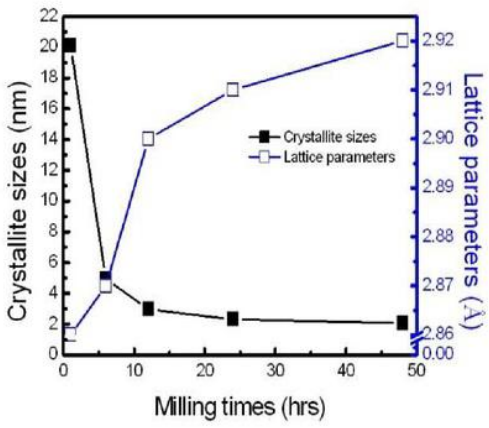

Fig. 3: Variations of the crystallite size and lattice parameters as functions of the milling time.

Figure 2, XRD patterns are obtained from the $Fe_{55}Mn_{35}Al_{10}$ nanocrystalline and amorphous alloys with different milling times. The 1-hr milled sample consists of mixed phase, such as bcc-Fe, bcc-Mn and fcc-Al. The Al and Mn diffraction peaks rapidly weaker after 1-hr milling while the remaining Bragg peaks from the bcc-Fe phases are becoming weaker and broader as the milling time increased. It could be assumed that the amorphization of Al and Mn occurs and the deformation of Fe structure starts undergoing fracture and welding, repeatedly. With further milling time, the Mn and Al peaks disappeared while the Fe peaks still remained. With the increasing of milling time (t_m), the $Fe_{55}Mn_{10}Al_{35}$ peaks of XRD patterns become weaker and broader, which correspond to the deformation of structure and variation in the particle size. It is shown that the alloying was activated after 6 hrs milling and both of nanocrstalline and amorphous were

discovered after 24-hr and 48-hr milling. One can see all the peaks after 6 hrs milling are broader and shifted to smaller angles, which are due to the deformation of the structure and variation in the crystallite size. The deformation is due to the replacement of the Fe atoms by Al and Mn atoms, which are the indication that an alloy has began to form. It means that the Al and Mn atoms are diffused into the Fe structure. After 48-hr milling, the deformed peak is look like a single crystal, and only one peak is still exist. It means that the sample is become amorphous.

Based on these XRD data, the crystallite size and the lattice parameter (*a*) can be evaluated from the Scherrer and Bragg equations, Figure 3. The crystallite size and lattice parameter based on Fe(110) peaks with respect to the milling time for $Fe_{55}Mn_{35}Al_{10}$ nanocrystalline and amorphous alloys. As a result, the sample alloyed until 48 hrs shows a bcc phase and the estimated crystallite size is around 20 to 2 nm and the lattice parameter is around 2.86 to 2.92 Å. We can see that the variation of the crystallite size and the lattice parameter based on Fe(110) peak with respect to the milling time is reasonable, the crystallite size decreased and the lattice parameter increased as the milling time is increased. The local structure and the atomic ordering were examined also by using EXAFS experiment. Variations of EXAFS spectra are related to the structural changes of alloys at the atomic scale. Mostly, the reduction of the amplitude of EXAFS spectrum is caused by the disorder in local structure. The phase shift of EXAFS spectrum is related to the change of chemical order [9]. Figure 4 shows *k*-weighted EXAFS spectra for mechanically-alloyed $Fe_{55}Mn_{35}Al_{10}$ for different milling time of 1, 6, 12, 24, and 48 hrs, respectively. The decrease of the amplitude until 6-hrs milling indicates that the fracture and the cold welding of Fe, Mn and Al were dominant and there was a minor change in the local structure. However, the significant changes in the amplitude and the phase took place after 12-hrs milling. This indicates that the alloying was dominant and new phases were formed after 12-hrs milling. The amount of the new phases increased as the processing time increased. It seems that the amount of the diffusion of Al and Mn atoms into the Fe structure increased gradually as the milling time increased. Especially, for the 48-hrs milled spectra near the value of k = 2.3 A^{-1} the spectrum patterns are different from the others. It means that the amorphous alloy was occurred in long range ordering. These results are in good agreement with the XRD results.

The radial atomic density in real space can be seen in the Fourier transformed spectrum. The peaks of the Fourier transformed spectra have the local structural information, such as the coordination number and the bonding distance, and the information on the vibration of neighboring atoms [10]. Figure 5 shows the Fourier transform of the EXAFS spectra measured at the Fe K-edge. The vertical dot lines indicate the first, second, third, and fourth shells of pure Fe which served as the guide lines (for alloyed samples to be compared). Based on the spectra, it is shown that the structure of the alloy is a bcc structure, also in a good agreement with Fe spectrum. As shown in Figure 5, the intensity of the shell peak in the Fourier transformed spectra gradually decreased with increasing the milling time.

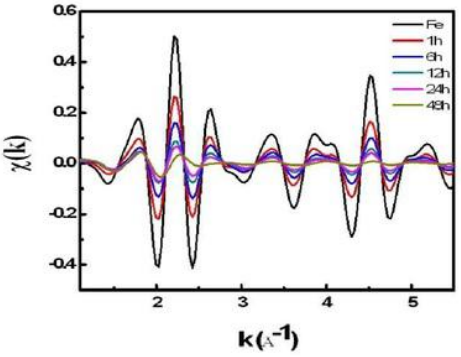

Fig. 4: *k*-weighted EXAFS spectra.

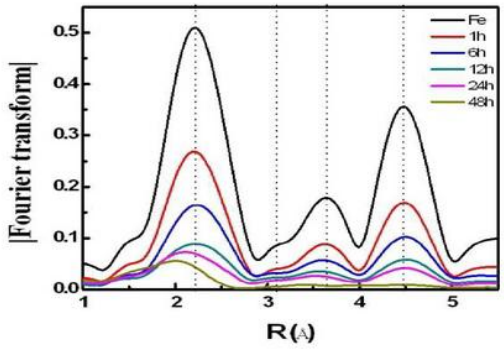

Fig. 5: Fourier transformed EXAFS spectra.

This indicates that the number of Fe–Fe direct bonds was decreased due to the diffusion of Mn and Al atoms into the bcc Fe shells. After 12-hr milling, the shift of the first shell peak represents the change of local structure around the Fe atoms due to formation of alloys respect to milling time. The substitution of Fe atoms by Mn and Al atoms increased as the milling times increased. The third shell peaks showing the long-range order in Fe-Fe in the Fourier transform of EXAFS spectra also decreased and shifted to longer atomic distances. This indicates that the long range order also reduces with the increase of themilling time. The higher shell peaks exhibit the long-range order in the Fe–Fe alloy in the Fourier transform of EXAFS spectra until 24-hrs milling. The higher shell peaks also gradually reduced up to a processing time which corresponds to the reduction of the long-range order. The 24-hrs milled sample exhibits the quite different position in the first shell with compare to the 1-hr milled sample. It can be explained that the Fe-Fe ordering was changed to Fe-Mn and Fe-Al order, indicating the alloy formation. One we can see also for the sample with 48-hrs milling, only the short-range order atoms were remained, the long-range ordering structures disappeared. It means that with the 48-hrs milling the sample becomes an amorphous.

Concerning the magnetic behaviors, both magnetization saturation (M_s) and coercivity (H_c) depend strongly on t_m. The M_s is decreased because thereis a decrease in the particle size and a change in the composition of a mixed powder, the transition from Fe, Al and Mn grains to $Fe_{55}Mn_{10}Al_{35}$ grains. This variation could be come from the

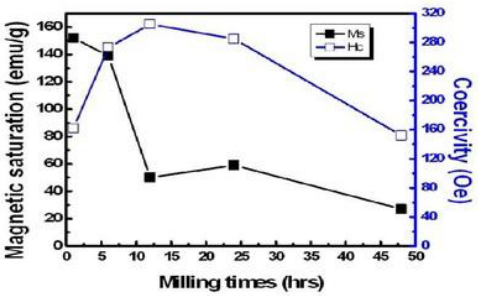

Fig. 6: Variations of magnetization saturation and coercivity to the milling time.

dilution of magnetic lattice of Fe which is caused by Mn and Al as increasing t_m. Meanwhile, H_c is found to increase with increasing t_m, which is assigned to a reduction in the crystallite size in single domain regimes. Figure 6 shows M_s and H_c for $Fe_{55}Mn_{35}Al_{10}$ alloys as a function of the milling time. We can see that M_s rapidly decreases in the range of 1 - 12 hrs because changes in the structure of mixed powder from Fe grains to $Fe_{55}Mn_{35}Al_{10}$ grains occur [11,12]. Starting from 12-hrs milling and afterwards, M_s slightly decreased. This variation of M_s is due to the saturation of the dilution of the magnetic lattice of Fe caused by Mn and Al. In Figure 6, one can also see that the H_c increases with the increasing of the milling time, reaching a maximum value at about 300 Oe after 12-hrs milling, and it decreases to about 150 Oe after 48-hrs milling. The H_c increase for a relatively short milling time can be attributed to a reduction in the crystallite size. Meanwhile, the decreases in H_c for a longer milling time indicate an increased formation of the Fe-Mn-Al alloy. Further milling times tended to make all samples highly disordered, then, they lost part of their high magnetic anisotropy, and H_c was reduced [13]. Furthermore, one can see from Fig. 3 and Fig. 6 that M_s is decreased while the lattice parameter increases.

Conclusion

The formations of $Fe_{55}Mn_{10}Al_{35}$ nanocrystalline and amorphous alloys were explicitly shown in the XRD patterns with shifted and broadened peaks. EXAFS spectra showed variations in the amplitude and the phase for the samples with milling time of 12 hrs and afterwards. The significant change in the structural phase confirmed that Al and Mn atoms were introduced to the Fe host lattice during the mechanical milling process. In the amorphous state the atoms of long-range order were disappeared. The $Fe_{55}Mn_{10}Al_{35}$ alloy is a good agreement with phase diagram of the ternary Fe-Mn-Al system by Chakrabarti as a ferromagnetic with the bcc structure. M_s was decreased due to the magnetic dilution caused by the incorporation of Al and Mn. Meanwhile, H_c decreased due to the development of single domains and the reduced particle size.

Acknowledgments

This research was supported by Basic Science Research Program through the National Research Foundation of Korea (NRF) founded by the Ministry of Education, Science and Technology (2010-0013155).

References

[1] R. Hasegawa, Present status of amorphous soft magnetic alloys, J. Magn. Magn. Mater. 215–216 (2000) 240-245.

[2] R. Hasegawa, Advances in amorphous and nanocrystalline magnetic materials, J. Magn. Magn. Mater. 304 (2006) 187–191.

[3] G. A. Perez Alcazar, J. A. Plascak, and E. Galvao da Silva, Magnetic properties of Fe-Mn-Al alloys in the disorder phase, Phys. Rev. B, vol. 4, (1988) 2816-2819.

[4] Heiko Bremers, Michael Fricke, and Jurgen Hesse, Structure and magnetic properties of FeMnAl alloys investigated by Mossbauer spectroscopy and X-ray diffraction, Hyperfine. Interact. 94 (1994) 1855-1859.

[5] M. M. Rico, Liga E. Zamaro, G. A. Peres Alcazar, J. M. Gonzalez, and A. Hernando Jr., Magnetic and Structural Study of Mechanically Alloyed $Fe_{0.7-x}Mn_xAl_{0.3}$, phys. Stat. sol. (b) 220, 445 (2000) 445-448

[6] M. M. Rico, G. Medina, G. A. Perez Alcazar, J. S. Munoz, S. Surinach, and M. D. Baro, Magnetic and Structural Properties of Mechanically Alloyed $Fe_x\ Mn_{0.70-x}\ Al_{0.30}$ (x = 0.40 and 0.45)Alloys, phys. stat. sol. (a) 189, No. 3, (2002) 811–816.

[7] J. Restrepo, G. A. Perez Alcazar, J. M. Gonzalez, Magnetic properties of disordered $Fe_{0.9-x}Mn_{0.1}Al_x$ alloys, J. Appl. Phys. Vol. 87 no. 10 (2000) 7425-7429.

[8] A.F. Rebolledo, J.J. Romero, R. Cuadrado, J.M. Gonzalez, F. Pigazo, F.J. Palomares, M.H. Medina, G.A. Perez Alcazar, Magnetic properties of ball-milled $Fe_{0.6}Mn_{0.1}Al_{0.3}$ alloys, J. Magn. Magn. Mater. 316 (2007) e418–e421.

[9] D.S. Yang, I. Kim, Y.-G. Yoo, B. Jiang, S.-G. Min, and S.-C. Yu, "EXAFS study for a magnetic shape memory alloy Ni-Mn-Ga," J. Kor. Phys. Soc., vol. 50 (2007) 1078–1083.

[10] D. S. Yang, I. Kim, Y.-G. Yoo, and S.-C. Yu, "EXAFS study for mechanically alloyed CoC ," J. Phys. Soc. Japan, vol. 71 (2002) 487–490.

[11] H. Shokrollahi, The magnetic and structural properties of the most important alloys of iron produced by mechanical alloying, J. Mater. Des. 30 (2009) 3374-3387.

[12] Kontan Tarigan, Yong-Goo Yoo, Dong-Seok Yang, J. M. Grenèche, and Seong-Cho Yu, Local Ordering Study of Nanostructure FeMnAl Alloys, IEEE Trans. Mag., vol. 45, No. 6 (2009) 2492-2495.

[13] J. Sort, S. Surinach, J. S. Munoz and M. D. Baro, J. Nogues, G. Chouteau, V. Skumryev and G. C. Hadjipanayis, Improving the energy product of hard magnetic materials, Phys. Rev. B 65 (2002) 174420-1 - 174420-5

Advanced Materials Research QiR 12
doi:10.4028/www.scientific.net/AMR.277

Local Structure and Magnetic Properties of FeMnAl Nanocrystalline and Amorphous Alloys

doi:10.4028/www.scientific.net/AMR.277.100

Local Structure and Magnetic Properties of FeMnAl Nanocrystalline and Amorphous Alloys

ORIGINALITY REPORT

19%	12%	14%	%
SIMILARITY INDEX	INTERNET SOURCES	PUBLICATIONS	STUDENT PAPERS

MATCH ALL SOURCES (ONLY SELECTED SOURCE PRINTED)

1%

★ K. Vallal Peruman. "Annealing effect on phase transformation in nano structured Ni-Mn-Ga ferromagnetic shape memory alloy", Phase Transitions, 07/2010

Publication

Exclude quotes	Off	Exclude matches	Off
Exclude bibliography	Off		